

Magnetoresistance Oscillations in Granular Superconducting Niobium Nitride Nanowires

U. Patel^{1, 2}, Z. L. Xiao*^{1, 2}, A. Gurevich³, S. Avci¹, J. Hua^{1, 2}, R. Divan⁴,

U. Welp², and W. K. Kwok²

¹ Department of Physics, Northern Illinois University, DeKalb, Illinois 60115

² Materials Science Division, Argonne National Laboratory, Argonne, Illinois 60439

³ National High Magnetic Field Laboratory, Tallahassee, Florida 32310

⁴ Center for Nanoscale Materials, Argonne National Laboratory, Argonne, Illinois 60439

We report on magnetoresistance oscillations in superconducting NbN_x nanowires synthesized through ammonia gas annealing of NbSe_3 precursor nanostructures. Though the transverse dimensions of the nanowires are much larger than the superconducting coherence length, the voltage-current characteristics of these nanowires at low temperatures are reminiscent of one-dimensional superconductors where quantum phase slips are associated with the origin of dissipation. By contrast, we show that both the magnetoresistance oscillations and voltage-current characteristics observed in this work result from the granular structure of our nanowires.

PACS numbers: 74.25.Fy, 74.25.Qt, 74.78.Na

Superconducting nanowires have recently received intense attention¹⁻¹⁵. On one hand, they are highly desirable in future electronic nanodevices. For example, nanowires of zero-resistance are ideal interconnects since they can circumvent the damaging heat produced by energy dissipation in a normal nano-conductor whose high resistance is inversely proportional to its cross-section area. Furthermore, in the resistive state they can also act as superconducting quantum interference devices^{9,10}. On the other hand, superconducting nanowires provide unique experimental testbeds to investigate and discover novel superconducting phenomena in confined geometries: Falk et al. probed dynamics of a few-row vortex lattice in NbSe₂ nanowires¹⁵ and Tian et al. reported an anti-proximity effect in Zn nanowires with bulk superconducting electrodes¹². Quasi one-dimensional (1D) superconducting nanowires with diameters comparable to the zero-temperature superconducting coherence length ξ_0 have been the research subject of thermal and quantum phase slip phenomena which induce dissipation at temperatures near and away from the superconducting critical temperature, respectively.

The observation of quantum phase slips (QPS) associated with the long resistance tail in the resistance versus temperature ($R-T$) curves at low temperatures is of significance not only for 1D superconductor but also for understanding the decoherence of a quantum system due to interaction with their environment¹⁴. However, interpretation of these results can be flawed by the presence of granularity in the nanowires that could give rise to a similar temperature dependence of the resistance^{4,7,13,16}. In fact, long resistance tails were observed in large NbTi nanowires and attributed to quantum collective creep of vortex lines³. It has also been demonstrated that the broadening of the superconducting transition can be induced by the size dependence of the critical temperature in the wire and/or even by the contact electrodes if they are made of the same material as the wire¹⁷.

In this Letter we report experiments on *free-standing* superconducting NbN_x nanowires which are stable in ambient atmosphere, enabling the attachment of gold electrodes for standard four-probe measurements. We observed intriguing magnetoresistance oscillations, which we attribute to the granular nature of the nanowires. More importantly, in addition to the long tail in the $R-T$ curves, we observed specific characteristics in voltage-current ($V-I$) measurements which resemble those^{2,13} reported in 1D superconductors where QPS were believed to be the origin for the low temperature dissipation. Since the transverse dimensions of our NbN_x nanowires are much larger than ξ_0 and both the resistance tail in the $R-T$ curves and the $V-I$ characteristics can be attributed to the granular nature of the nanowires, our results highlight the complexity of probing QPS in superconducting nanowires.

NbN_x nanowires with critical temperatures up to 11 K and transverse dimensions down to tens of nanometers were synthesized by annealing NbSe_3 nanostructure precursors in flowing ammonia gas at temperatures up to 1000°C [Ref.18]. By utilizing standard photolithography and lift-off process, four gold electrodes with a gap of 5 μm between voltage leads were deposited onto individual nanowires by magnetron sputtering. We carried out angular dependent DC magneto-transport measurements in the constant current mode in a magnet-cryostat system which enabled precise stepper-motor controlled sample rotation in a magnetic field. Data reported here are from two NbN_x wires with widths and thicknesses of $w = 350$ nm, $d = 160$ nm (sample A) and $w = 500$ nm, $d = 320$ nm (sample B), respectively. The zero-field critical temperature T_{c0} defined with a 50% normal state resistance R_N criterion is 9.94 K and 7.25 K for samples A and B, respectively.

The main panels and the upper-left insets of Fig.1 present the essential finding of this research. In the low-field regime of the magnetic field dependence of the resistance ($R-H$) curves

we observe reproducible and pronounced oscillations in both samples. Similar magnetoresistance oscillations were observed in Nb-Ti/Cu multilayers in parallel magnetic fields and interpreted as the dynamic matching of a moving vortex lattice with the periodic microstructure¹⁹. However, we find significant differences between the data in multilayers and ours: the magnetoresistance oscillations in multilayers persist up to the normal state while in our samples they occur only at low dissipation levels (less than 20% R_N) and in the low field regime where the change of the magnetoresistance is relatively weak. More importantly, the dynamic matching induced oscillations¹⁹ disappear at low driving currents, in contrast to the data presented in Fig.2(a) which show that the amplitude of the oscillation decreases with increasing current.

Figure 2(b) presents the fast Fourier transform (FFT) power spectrum of the magnetoresistance of sample A at 9.2 K. The FFT spectrum indicates that the magnetoresistance oscillation is quasi-periodic, the dominant peak at $f = 55 \text{ T}^{-1}$ in the FFT spectrum corresponding to a period of $\Delta H = 0.018 \text{ T}$. Similarly we obtained a period of $\Delta H = 0.013 \text{ T}$ for the dominant oscillation in the R - H curves of sample B.

The observed oscillation periods are consistent with two physically different field scales, which turn out to be of the same order of magnitude. The first one is the lower critical field H_{c1} in a thin film strip of width w smaller than the London penetration depth, λ . For NbN_x, $\lambda(0)$ at zero temperature is about 200 nm. Thus, for sample A ($T_{c0} = 9.94\text{K}$) at $T \geq 9\text{K}$ and, we have $\lambda(T) = \lambda(0)[T_{c0}/(T_{c0}-T)]^{1/2} \geq 650 \text{ nm} > w$. In this case $H_{c1} \approx (2\Phi_0/\pi^2 w^2)\ln(w/\xi)$ where Φ_0 is the flux quantum²⁰ sets the field increment required for penetration of the first few vortex rows resulting in resistance and magnetization oscillations²¹. For $w = 300 \text{ nm}$ and $w/\xi = 100$ characteristic of our nanowires, $H_{c1} \approx 20 \text{ mT}$ is consistent with the oscillation periods in Fig.2(b). Given the rough edges of NbN nanowires, one can hardly expect an ideal penetration of parallel vortex rows, but

rather penetration of mesoscopic vortex segments through different regions of suppressed edge barrier along the nanowire. The incoherent penetration of such vortex bundles can produce resistive oscillations characterized by a distribution of nearly temperature independent periods $\sim H_{c1}$, in agreement with our data. However, both theories^{21,22} and experiments^{21,23} demonstrate that the period of the oscillation originating from the vortex rearrangement should increase with increasing number of vortex rows. This differs from our data which show no change of the period with increasing field.

Another mechanism of oscillations can result from the granular structure of the nanowires which was proposed by Herzog et al. to explain the magnetoresistance oscillations observed in their *in-situ* grown granular Sn nanowires: screening currents circulating around phase coherent loops of weakly linked superconducting grains⁵. In this case the transport is limited by critical currents I_c across the grain boundaries (GB), which can be treated as short ($w < \lambda$) Josephson junctions. Such GB network can also produce the magnetotransport oscillations determined by the Fraunhofer oscillations of $I_c(H)$ through a thin film Josephson junction of length L . Such oscillations have the field period, $\Delta H \approx 1.8\Phi_0/L^2$ [Ref.24]. In a narrow nanowire, the distribution of GB lengths $L = w/\cos\alpha$ of straight GBs spanning across the entire cross section is determined by the distribution of local angles α between a GB and the edge of the nanowire. For $w = 300$ nm, we obtain $\Delta H_i = 40\cos^2\alpha_i$ mT, consistent with the magnitude and the temperature independence of the oscillation periods. Additional resistance harmonics with smaller field periods may result from spatial inhomogeneities along GBs, for example, faceting²⁵ and penetration of first vortex rows. As the field increases, further flux penetration in the grains washes out the Fraunhofer oscillations, resulting in two distinct regimes in a $R-H$ curve and apparent oscillations occur in the low-field weak magnetoresistance regime. It is also

understandable that the nanowires are granular since the replacement of Se atoms by N atoms during the conversion from NbSe_3 to NbN_x at high temperatures will cause atomic scale rearrangements, resulting in a change in the morphology of the nanowire. In fact, both AFM (see inset of Fig.2(a)) and SEM images revealed the granular morphology of the NbN_x nanowires with an average grain size of 20-30 nm and also showed the existence of tiny voids¹⁸.

Experiments on the magnetic field orientation effect on the resistance oscillation also provide strong support for the above interpretation. The inset of Fig.3(a) presents R - H curves obtained with the magnetic field applied at angles from perpendicular ($\phi = 0^\circ$) to parallel ($\phi = 90^\circ$) to the wire axis. Oscillations can be seen in all R - H curves and the period increases when the applied field is tilted towards the wire axis. The angular dependence of the oscillation period can be understood given the fact that only the perpendicular component of the magnetic field can penetrate GBs, thus, the period ΔH should increase as $1/\cos\phi$. Indeed, this dependence was revealed by the experimental data plotted in the main panel of Fig.3(a) for the dominant period. Considering that a loop of intragranular screening current may not be precisely contained in the x - I plane, the fitting and the experimental data are reasonably consistent. Data given in Fig.3(b) provide further evidence: the same tendency is also observed for the oscillations in R - H curves with the magnetic field rotating in the plane perpendicular to the wire axis. In this case the oscillation period or the first peak field H_1 as defined in the inset again follows the relation $\sim 1/\cos\theta$ at angles up to 70° .

As we mentioned above, there has been a long running debate on the origin of the resistance tail in R - T curves of quasi 1D superconducting nanowires, since both QPS and granularity of the nanowires can induce similar effects. Both analysis of the nanowire morphology and magnetoresistance oscillations revealed that our NbN_x nanowires are granular. The R - T curves

presented in the lower-right insets of Fig.1 also indicate that their granularity (coupling between grains) is adjustable: the transition widths measured between 10% and 90% of R_N are 0.66 K and 2.65 K for samples A and B, respectively. The normal state resistivity of sample B ($10.6 \text{ m}\Omega\cdot\text{cm}$) is about 50 times larger than that of sample A ($0.2 \text{ m}\Omega\cdot\text{cm}$). Inset of Fig.4(b) also shows that the $R-T$ curve of sample B has a long resistance tail with an exponential decay similar to those observed in thin Sn nanowires¹³. Thus NbN_x nanowires serve as a good model system for probing superconducting granular properties in larger nanowires, providing a benchmark to reveal the origin of the resistive dissipation in superconducting nanowires.

Figures 4(a) and (b) show features in $V-I$ characteristics of NbN_x nanowires similar to those^{2,13} observed in quasi 1D superconducting nanowires where QPS is believed to contribute to the dissipation: ohmic finite resistance at low currents appearing at temperatures far way from T_c in sample B which has weaker grain coupling resembles those found in smaller diameter (40 nm and 20 nm) Sn nanowires¹³. Although the voltage jumps and steps observed in $V-I$ curves of our samples resemble those found in small Sn nanowires, the similarity can be attributed to the self-heating effect which naturally occurs in granular nanowires. In fact, as presented in the inset of Fig.4(a) the current I^* where the first voltage jump occurs follows the square root temperature dependence predicted by the self-heating model²⁶. As shown by the $V-I$ curve obtained at 2 K for sample A, similar voltage ‘flip-flop’ as that reported in Sn nanowires with diameter of 70 nm also occurs in our NbN_x granular nanowires. The ‘flip-flop’ can be a result of sample inhomogeneity: the nanowire may contain a normal channel which serves as a shunt resistor and introduces a quasi-ohmic voltage bias to the system, inducing a self-heating voltage oscillation within a certain current range²⁷. Furthermore, Giordano et al. observed oscillatory structure in $V-I$ curves in 1D PbIn wires and explained it with the quantum tunneling rate change due to the

current dependence of the quantum levels². This oscillatory structure can even evolve into a voltage minimum, as reported by Tian et al. in their thinnest Sn nanowires¹³. As shown in Fig.4(b), similar structures including the voltage minimum also appear in V - I curves of our NbN_x nanowires at low temperatures. In a granular nanowire, this can be explained by the increase in the quasiparticle tunneling rate due to the suppression of superconductivity in the grains arising from current induced depairing and/or self-heating²⁸.

In summary, we observed magnetoresistance oscillations in *free-standing* superconducting NbN_x nanowires. Our experiments have shown that these oscillations can result from the Fraunhofer oscillation of intergranular critical currents. We also found that the granularity of the nanowire can induce similar features in the voltage-current characteristics as those commonly attributed to quantum phase slips.

This material is based upon work supported by the US Department of Energy Grant No. DE-FG02-06ER46334 and Contract No. DE-AC02-06CH11357. S. A. was supported by the National Science Foundation (NSF) Grant No. DMR-0605748. The nanocontacting and morphological analysis were performed at Argonne's Center for Nanoscale Materials (CNM) and Electron Microscopy Center (EMC), respectively.

*Corresponding author, xiao@anl.gov or zxiao@niu.edu

References

- [1]. N. Giordano, Phys. Rev. Lett. **61**, 2137 (1988).
- [2]. N. Giordano and E. R. Schuler, Phys. Rev. Lett. **63**, 2417 (1989).
- [3]. X. S. Ling et al., Phys. Rev. Lett. **74**, 805 (1995).
- [4]. P. Xiong, A. V. Herzog, and R. C. Dynes, Phys. Rev. Lett. **78**, 927 (1997).
- [5]. A. V. Herzog, P. Xiong, and R. C. Dynes, Phys. Rev. B **58**, 14199 (1998).
- [6]. A. Bezryadin, C. N. Lau, and M. Tinkham, Nature **404**, 971 (2000).
- [7]. C. N. Lau et al., Phys. Rev. Lett. **87**, 217003 (2001).
- [8]. D. Y. Vodolazov et al., Phys. Rev. Lett. **91**, 157001 (2003).
- [9]. A. Johansson et al., Phys. Rev. Lett. **95**, 116805 (2005).
- [10]. D. S. Hopkins et al., Science **308**, 1763 (2005).
- [11]. A. Rogachev, A. T. Bolinger, and A. Bezryadin, Phys. Rev. Lett. **94**, 017004 (2005).
- [12]. M. L. Tian et al., Phys. Rev. Lett. **95**, 076802 (2005).
- [13]. M. L. Tian et al., Phys. Rev. B **71**, 104521 (2005).
- [14]. F. Altomare et al., Phys. Rev. Lett. **97**, 017001 (2006).
- [15]. A. Falk et al., Phys. Rev. B **75**, 020501 (2007).
- [16]. J. M. Duan, Phys. Rev. Lett. **74**, 5128 (1995).
- [17]. M. Zgirski and K. Yu. Arutyunov, Phys. Re. B **75**, 172509 (2007).
- [18]. U. Patel et al., Appl. Phys. Lett. **91**, 162508 (2007).
- [19]. A. Gurevich, E. Kadyrov, and D. C. Larbalestier, Phys. Rev. Lett. **77**, 4078 (1996).
- [20]. A.A. Abrikosov, Zh. Exp. Teor. Fiz. **46**, 1464 (1964) [Sov. Phys. JETP **19**, 988 (1964)].
- [21]. S. H. Brongersma et al., Phys. Rev. Lett. **71**, 2319 (1993); G. Carneiro, Phys. Rev. B **57**, 6077 (1998).

- [22]. C. Hunnekes et al., Phys. Rev. Lett. **72**, 2271 (1994).
- [23]. J. Eisenmenger et al., Physica C **411**, 136 (2004).
- [24]. P.A. Rosenthal et al., Appl. Phys. Lett. **59**, 3482 (1991); M. Moshe, V.G. Kogan, and R.G. Mints, Phys. Rev. B **78**, 020510 (R) (2008).
- [25]. X. Y. Cai et al., Phys. Rev. B **57**, 10951 (1998).
- [26]. A.V. Gurevich and R. G. Mints, Rev. Mod. Phys. **59**, 941 (1987).
- [27]. A. Wehner et al., Phys. Rev. B. **63**, 144511 (2001).
- [28]. A. Gerber et al., Phys. Rev. Lett. **65**, 3201 (1996).

Figure captions

FIG.1 (Color online). R - H curves of samples A ($I=2 \mu\text{A}$) and B ($I=0.5 \mu\text{A}$). Upper-left insets show expanded views of the low-field data at numerous fixed temperatures. The magnetic field direction is perpendicular to the wire axis. Zero-field R - T curves are given in the lower-right insets.

FIG.2 (Color online). (a) R - H curves of sample A at 9.2 K and various applied currents. Inset shows an AFM image of sample B. (b) FFT trace from R_{osc} - H curve presented in the inset for sample A at 9.2 K, where R_{osc} is the oscillatory part of the R - H curve at $I=2 \mu\text{A}$.

FIG.3 (Color online). Period of the dominant oscillation ΔH and the first peak field H_1 at various angles. The solid lines represent the inverse cosine relationship. The definitions of angles ϕ and θ are given in the lower-right insets. R - H curves at various angles are presented in the upper-left insets where the curves at angles other than 90° have been offset for clarity.

FIG.4 (Color online). V - I characteristics at various temperatures in zero field. The inset in (a) gives the temperature dependence of the current I^* at which the first voltage jump occurs, where the solid symbols and line are experimental data and the fit, respectively. Inset of (b) presents the zero-field R - T curve of sample B with resistance in logarithmic scale.

FIG.1

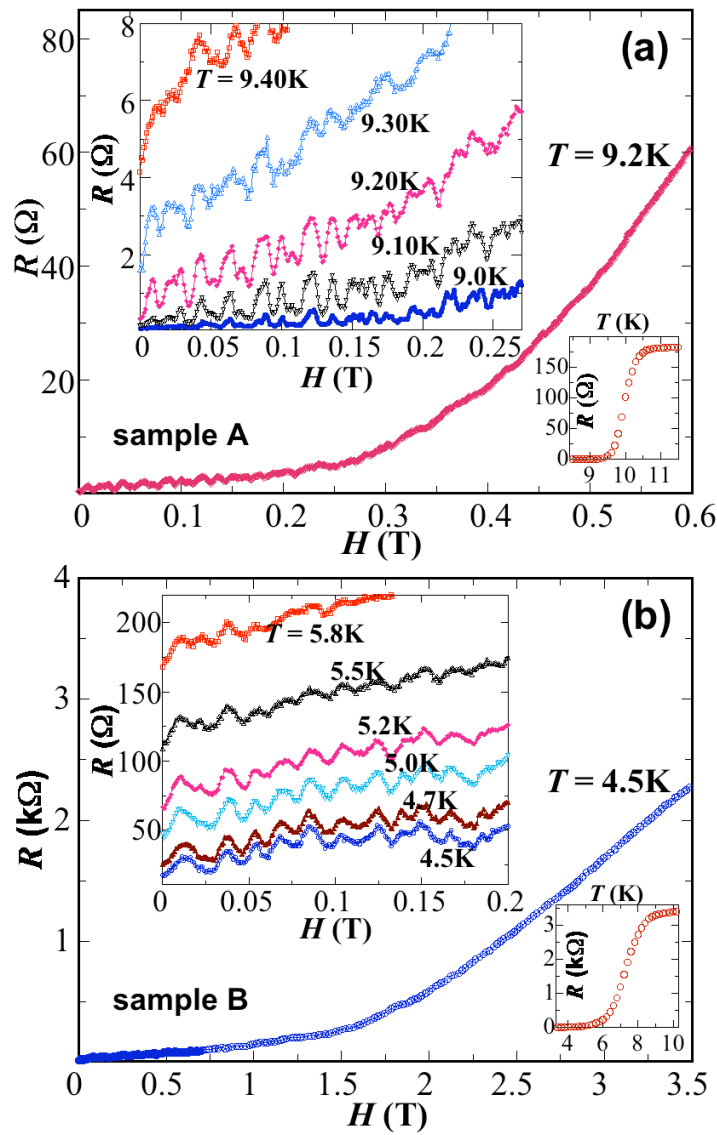


FIG.2

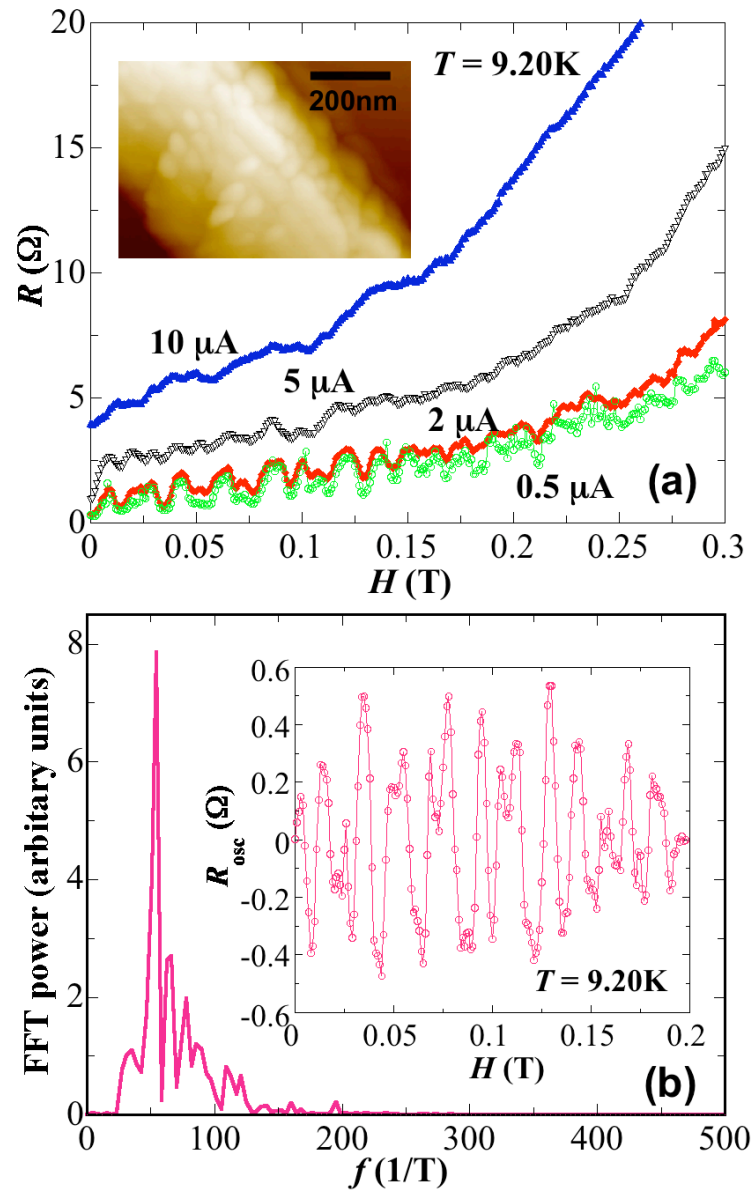


FIG.3

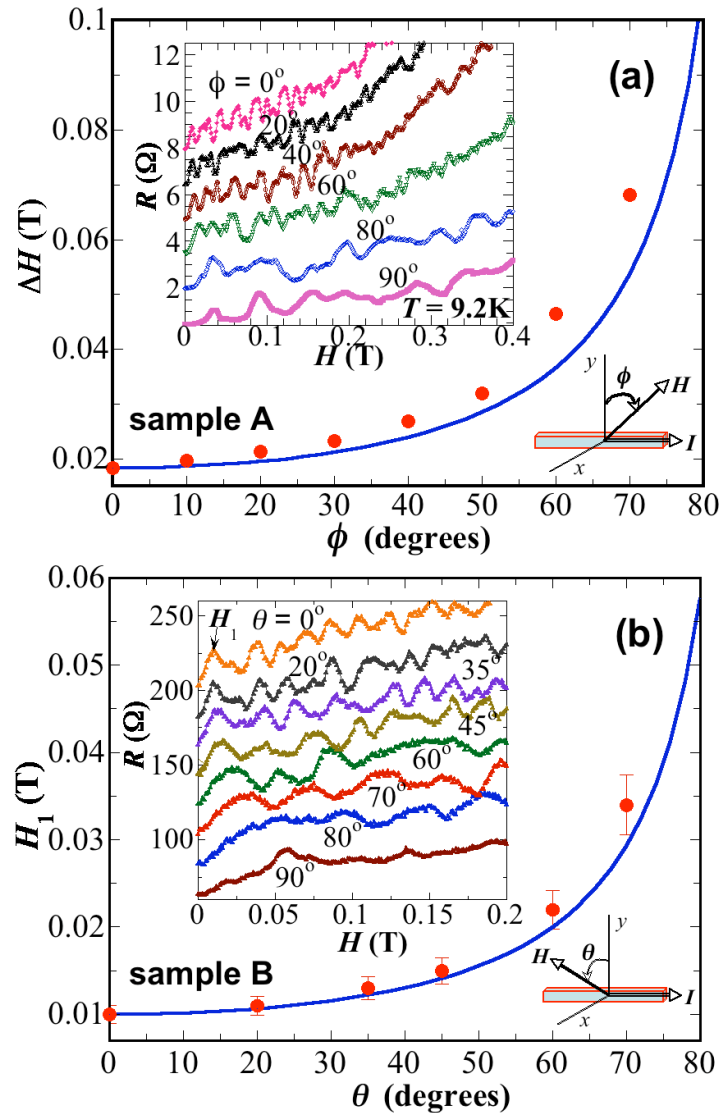


FIG.4

